Supersymmetry, half-bound states, and grazing incidence reflection

OPEN ACCESS
IOP Publishing
Journal of Optics
J. Opt. **23** (2021) 075602 (8pp)
https://doi.org/10.1088/2040-8986/ac01b1

Supersymmetry, half-bound states, and grazing incidence reflection

D A Patient* and **S A R Horsley**

School of Physics and Astronomy, University of Exeter, EX4 4QL Exeter, United Kingdom

E-mail: dp348@exeter.ac.uk

Received 4 December 2020, revised 12 April 2021
Accepted for publication 10 May 2021
Published 28 May 2021

Abstract

Electromagnetic waves at grazing incidence onto a planar medium are analogous to zero energy quantum particles incident onto a potential well. In this limit waves are typically completely reflected. Here we explore dielectric profiles supporting optical analogues of 'half–bound states', allowing for zero reflection at grazing incidence. To obtain these profiles we use two different theoretical approaches: supersymmetric quantum mechanics, and direct inversion of the Helmholtz equation, showing that discretized approximations to these profiles exhibit low reflectivity close to grazing incidence.

Keywords: half bound states, no reflection at grazing, factorisation method & SUSY

(Some figures may appear in colour only in the online journal)

1. Introduction

At grazing incidence, a wave is nearly always completely reflected from a surface. The effect can be observed optically for almost any surface viewed at a shallow angle, where it behaves as a mirror. This behaviour has been known for a long time, and is used to enhance quantum reflection [1], and x-ray scattering (where the refractive index typically differs only slightly from unity) [2]. Conversely, it presents a problem for radar absorbers [3], and perfectly matched layers in numerical simulations [4]. In this work we investigate the problem of designing graded dielectric materials that do not reflect at grazing incidence.

Mathematically the phenomenon can be seen from a straightforward examination of the Helmholtz equation. For an electromagnetic (EM) wave incident at an angle $\cos(\theta) = k_x/\sqrt{\epsilon_b}k_0$ onto a graded dielectric profile $\epsilon(x)$, and in terms of the dimensionless coordinate $\xi = k_x x$, the Helmholtz equation is

$$\left[\frac{d^2}{d\xi^2} + 1 + \left(\frac{k_0}{k_x}\right)^2 (\epsilon(\xi) - \epsilon_b)\right] \phi(\xi) = 0 \tag{1}$$

where ϵ_b is the background value of the permittivity, such that $\epsilon(\xi) \to \epsilon_b$ as $|\xi| \to \infty$. These coordinates are scaled such that away from the inhomogeneity the wave takes the form $e^{\pm i\xi}$ irrespective of the angle of incidence. The effect of the angle is now subsumed in an effective permittivity profile $(k_0/k_x)^2\epsilon(\xi)$. This effective permittivity becomes infinitely large at grazing incidence, when $k_x \to 0$. A general permittivity profile will therefore act as a perfect reflector in this limit. As a concrete example, take the Fresnel coefficients for the transverse electric (TE) and transverse magnetic (TM) polarizations [5]

$$r_{TE} = \frac{\mu_2 k_{x,1} - \mu_1 k_{x,2}}{\mu_2 k_{x,1} + \mu_1 k_{x,2}}$$
$$r_{TM} = \frac{\epsilon_2 k_{x,1} - \epsilon_1 k_{x,2}}{\epsilon_2 k_{x,1} + \epsilon_1 k_{x,2}} \tag{2}$$

where the normal components of the wave–vectors are $k_{x,n} = \sqrt{\epsilon_n \mu_n k_0^2 - k_y^2}$. At grazing incidence $k_{x,1} \to 0$, it is clear from equation (2) that both TE and TM reflectivities tend to unity, as shown in figure 1(a). In figure 1(b) we show that this is also the case for an arbitrarily chosen dielectric profile (here a Gaussian variation of $\epsilon(x)$). Despite a low

* Author to whom any correspondence should be addressed.

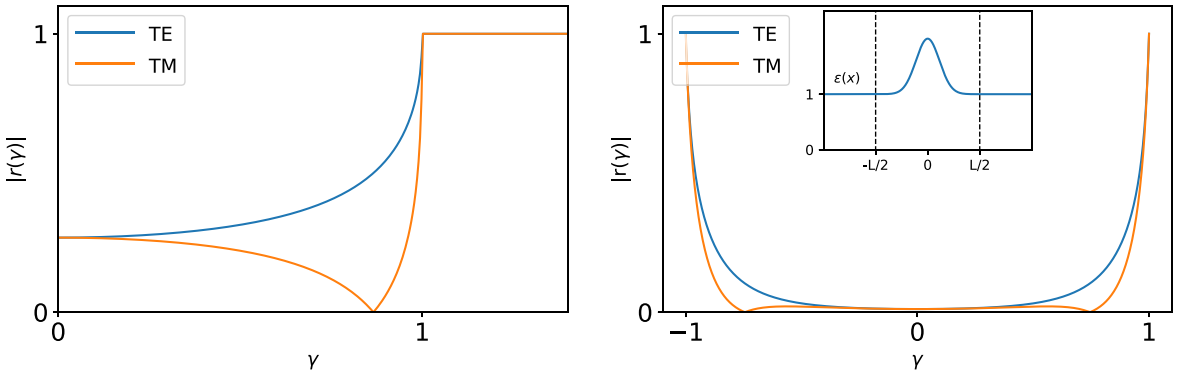

(a) Magnitude of Fresnel reflection coefficients ($\epsilon = 3$, $\mu = 1$) as a function of $\gamma = k_y/\sqrt{\epsilon_b}k_0$ for EM waves incident onto an interface between dielectric half spaces.

(b) Magnitude of the TE and TM reflection coefficients as a function of $\gamma = k_y/\sqrt{\epsilon_b}k_0$ for the arbitrarily chosen permittivity profile shown inset.

Figure 1. In general, as an EM wave approaches grazing incidence ($\gamma = k_y/\sqrt{\epsilon_b}k_0 = 1$) the reflectivity for both TE and TM waves approaches unity.

reflectivity of this smooth profile at normal incidence, the reflection nevertheless becomes complete at grazing incidence. One can picture this as analogous to a stone skimming on the surface of water. As the stone's momentum becomes close to parallel to the surface, only a small impulse is required to reverse the stone's motion normal to the surface.

Despite this general behaviour, surprisingly there are permittivity profiles (and analogous graded sound speeds in acoustics, or potentials $V(x)$ in quantum mechanics) that do *not* act as perfect reflectors at grazing incidence. The Pöschl–Teller potential [6] is perhaps the most famous example of such a non–reflecting profile: at some frequencies this potential does not reflect radiation at *any* angle of incidence, despite a potentially rapid spatial variation of the profile. This profile has been experimentally realised as a multilayer structure [7], and its non-reflecting behaviour is understood in terms of inverse scattering theory and the solitons of the Kortweg–de Vries equation [8–10]. Another example is provided by anisotropic magnetodielectric *transformation media* [11, 12] (where $\boldsymbol{\epsilon} = \boldsymbol{\mu}$), which enact an effective transformation of the coordinate system. Given this equivalence these materials cause no scattering whatsoever, for grazing incidence or otherwise. Finally, isotropic dielectric materials obeying the spatial Kramers–Kronig relations [13] also do not reflect any wave incident from one side, although the limit of grazing incidence is particularly delicate for these profiles, requiring them to be infinitely extended [14].

Here we take a different approach to design materials without reflection at grazing incidence. EM waves approaching an interface at grazing incidence are analogous to zero energy quantum particles incident onto a potential well. It is known that there exist threshold anomalies [15], due to presence of so–called half-bound states (HBSs) [15], allowing complete transmission through the potential well at zero energy [16]. The optical analogue of these anomalies therefore allow the complete transmission of grazing incidence waves. The naming of these HBSs originates in Levinson's theorem [17] (see [18] for a interesting review, and [19] for a simple proof), which connects the number of bound states of a potential to the phase shift of scattering in the zero energy limit. As the name suggests, HBSs count as half of a bound state in the phase shift. These states are non-normalizable 'bound' states with zero energy.

To find materials supporting these HBSs we take two theoretical approaches. The first is to apply the factorisation method [20] to the Helmholtz equation, similar to the factorization of the harmonic oscillator's Schrödinger equation into raising and lowering operators [21]. Requiring that the 'lowering' operator of this factorization has a zero eigenvalue we obtain a permittivity profile that does not reflect grazing incidence waves. This approach connects with recent work on analogues of supersymmetric quantum mechanics (SUSY) in optics [22–27], to design complex potentials [28, 29] and optical fibres [30] amongst other things, and where the same factorization is leads to isospectral structures. The difference between the isospectral structures is the removal of a single bound state. In our case that single state is a half bound state, which is what gives us zero reflection at grazing incidence.

In addition to factorization of the Helmholtz equation, we derive another set of permittivity profiles from an inversion of the Helmholtz equation, where the permittivity is written in terms of the wave amplitude. As we will see, this yields similar results to the factorization approach, but with the freedom to specify additional boundary conditions. As an example, we will derive a graded abosrbing dielectric layer that can be added to a mirror, which removes reflection at or close to grazing incidence.

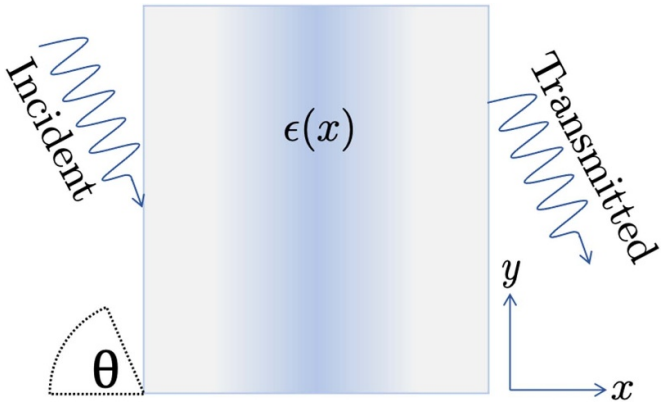

Figure 2. A wave propagating along the x-axis is incident onto a planar dielectric whose permittivity varies as $\epsilon(x)$. The dielectric structure $\epsilon(x)$ is chosen such that as the incident angle approaches $\pi/2$ from the x-axis (grazing incidence), there is no reflected wave.

2. Grazing incidence reflection and HBSs

We first review the problem of vanishing reflection at grazing incidence, and it is relation to so–called 'HBSs'. Consider a plane wave incident from the left of a dielectric profile $\epsilon(x)$, the profile becoming homogeneous as $|x| \to \infty$, as in figure 2. For zero reflection, the wave must be of the form $\exp(ik_x x)$ on the far left and far right of the profile. Outside the slab the Helmholtz equation becomes, in the limit of grazing incidence, Laplace's equation $d^2\phi/dx^2 = 0$ with solutions $a + bx$, where a and b are constants. But if there is to be zero reflection in this limit, outside the slab we must have $\exp(ik_x x) \to 1 + ik_x x$. As $k_x \to 0$ the wave equals unity everywhere outside the slab. Therefore if there is to be zero reflection in the limit of grazing incidence the Helmholtz equation must have two independent solutions, one which is equal to a constant on both sides of the slab, and the other proportional to the x coordinate, with the same proportionality constant on both sides of the slab. Provided the permittivity profile is symmetric about its centre (so that both $\phi(x)$ and $\phi(-x)$ are solutions), and that one of the solutions to the TE field is constant outside the slab, we thus ensure zero reflection at grazing incidence (although non–symmetric potentials can also exhibit less than complete reflection at grazing [31]). In quantum mechanics a state which is constant outside of a potential where it is 'bound' is not normalizable, and is known as a 'HBS' (see e.g. page 280 of [32] for a classification of the bound states of potentials). These states are bound states with an energy that is at the edge of the continuum. In the reflection from a dielectric profile we can understand these states as wave–guide modes whose decay constant is close to zero. From this point of view we are providing a method for designing waveguides with one mode with vanishing decay constant outside the guide.

The simplest example of a system supporting a HBS is a homogeneous slab waveguide of width L, with a constant permittivity $\epsilon(x) = \epsilon$ that spans a region $x \in [-L/2, L/2]$. Re–introducing the coordinate x, equation (1) becomes

$$\left[\frac{d^2}{dx^2} + k_0^2\left(\epsilon(x) - \epsilon_b\right) + k_x^2\right]\phi(x) = 0, \tag{3}$$

The solutions within the two regions are respectfully given by $\phi(x) = \exp(\pm\ \mathrm{i}k_x x)$ $(|x| > L/2)$ and $\phi(x) = \exp(\pm \mathrm{i}\sqrt{k_0^2(\epsilon - \epsilon_b) + k_x^2}\,x)$ $(|x| < L/2)$. If the phase accumulated inside the slab is an integer number of π, the field on the right of the slab is $\pm$ the field on the left, and the boundary conditions can be fulfilled without any reflected wave. This condition is given by

$$\exp\left[\pm\mathrm{i}\sqrt{k_0^2(\epsilon - \epsilon_b) + k_x^2}L\right] = \pm 1 = \exp(\mathrm{i}n\pi), \tag{4}$$

a condition which can be fulfilled with a slab of length $L = n\pi/\sqrt{k_0^2(\epsilon - \epsilon_b) + k_x^2}$, which is the standard condition for a transmission resonance. If we choose the angle of zero reflection to be grazing incidence, then the slab waveguide must have width

$$L = \frac{n\pi}{k_0\sqrt{\epsilon - \epsilon_b}}. \tag{5}$$

In this case the field outside the slab reduces to a constant at grazing incidence, which is the HBS just mentioned. Figure 3 shows the numerically computed reflectivity as a function of angle for a homogenous slab of permittivity $\epsilon = 3$ and background permittivity $\epsilon_b = 1$ whose length satisfies equation (5). Here we apply the odeint function from the SciPy library [33] to integrate equation (3) and find the scalar field ϕ, from which we can compute the reflection coefficient outside the device as $r = (\phi - \phi'/\mathrm{i}k_x)/(\phi + \phi'/\mathrm{i}k_x)$. As the figure shows, the TE reflectivity is zero as we approach $|\gamma| = |\sin(\theta)| = 1$.

2.1. Factorisation method

In this section, we use the factorisation method usually applied in supersymmetric quantum mechanics [20] to design a family of HBS supporting dielectric profiles, which do not reflect TE waves at grazing incidence. We note that our approach connects with recent work in quantum mechanics by Ahmed *et al* where zero energy reflectionless potentials have been investigated in several cases [34–36], and where HBS supporting potentials have been subject to supersymmetric transformations to generate e.g. potentials supporting no bound states at all [37].

Here we start by writing the Helmholtz equation equation (3) for $k_x = 0$ as a product of first order operators

$$\left(-\frac{d}{dx} + k_0\alpha(x)\right)\left(\frac{d}{dx} + k_0\alpha(x)\right)\phi(x) = \hat{a}^\dagger\hat{a}\phi(x) = 0, \tag{6}$$

where $\hat{a}^\dagger, \hat{a}$ are analogous to raising and lowering operators in quantum mechanics (although their commutator is *not* proportional to a constant). Two forms of equation (6) are possible, depending on the order of $\hat{a}$ and $\hat{a}^\dagger$. We subsume these into a single 'super' equation, defining

$$\hat{Q}_- = \begin{pmatrix} 0 & \hat{a}^\dagger \\ 0 & 0 \end{pmatrix},\ \hat{Q}_+ = \begin{pmatrix} 0 & 0 \\ \hat{a} & 0 \end{pmatrix} \tag{7}$$

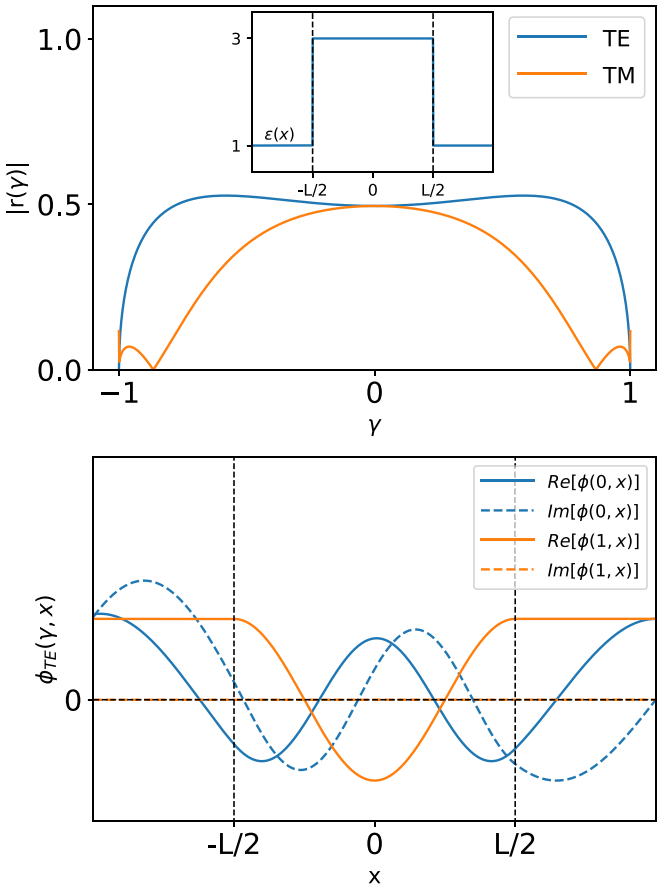

Figure 3. Reflectivity (top) as a function of incidence angle θ ($\gamma = \sin(\theta)$) for a homogeneous slab (permittivity profile inset) in free space ($\epsilon_b = 1$), whose length obeys equation (5) for $\epsilon = 3$, $k_0 = 1$ and $n = 2$. (bottom) The field of a TE wave incident onto the slab (boundaries indicated as vertical dashed lines), in the cases where the initial wave is at normal incidence (blue) and close to grazing (orange). At grazing incidence, the field decays to a non-zero constant outside the region where the dielectric exists, indicating that the slab supports a HBS.

so that

$$\hat{H}\psi = \left(\hat{Q}_+\hat{Q}_- + \hat{Q}_-\hat{Q}_+\right)\psi = \begin{pmatrix} \hat{a}^\dagger\hat{a} & 0 \\ 0 & \hat{a}\hat{a}^\dagger \end{pmatrix}\begin{pmatrix} \phi_1 \\ \phi_2 \end{pmatrix} = 0 \quad (8)$$

where ϕ_1 and ϕ_2 represent the two EM fields obeying the Helmholtz equations with the order of $\hat{a}$ and $\hat{a}^\dagger$ reversed. In supersymmetric quantum mechanics the operators $Q_\pm$ are called the supercharge operators, and commute with the Hamiltonian $[\hat{Q}_\pm, \hat{H}] = 0$.

The factorization (equation (8)) can only be carried out for certain forms of the permittivity $\epsilon(x)$. Assuming grazing incidence $k_x = 0$, expanding out the product in equation (8), and comparing to equation (3) gives the relationship between the function $\alpha(x)$, and the two possible material profiles $\epsilon(x)$

$$\epsilon_\pm(x) - \epsilon_b = \pm\frac{1}{k_0}\frac{d\alpha(x)}{dx} - \alpha^2(x). \quad (9)$$

Having factorized the Helmholtz equation in the form of equation (8), we can immediately find the solutions. The supercharge operators commute with the Hamiltonian, and therefore the solutions to $\hat{Q}_\pm\psi = 0$ are also solutions to $\hat{H}\psi = 0$. For instance, the solution to $\hat{Q}_\pm\psi = 0$ has $\phi_{2,1} = 0$ and

$$\phi_{1,2}(x) = \phi_{1,2}(-L/2)\exp\left[\mp k_0\int_{-L/2}^{x}\alpha(x')dx'\right], \quad (10)$$

which are the solutions for grazing waves incident onto the profiles $\epsilon_\pm$ given in equation (9). By inspection of equation (9), one can see that if $\alpha(x) \to 0$ as $|x| \to \infty$, then the permittivity tends to the background value $\epsilon(x) = \epsilon_b$, as required. As discussed earlier for vanishing reflection of grazing incidence waves, the amplitude of the wave outside of the slab must be the same on either side. This requires $\int_{-L/2}^{L/2}\alpha(x)dx = 0$, a condition which we enforce by choosing $\alpha(x)$ antisymmetric around $x = 0$.

In the case of a true bound state $\alpha(x)$ tends to a constant or diverges at infinity. If e.g. $\alpha > 0$ as $|x| \to \infty$ the solution to ϕ_1 (equation (10)), in the profile ϵ_+ exponentially decays as x becomes large. Meanwhile the solution ϕ_2 in ϵ_- diverges at infinity and is thus not a physically allowed solution to the equation. By contrast, here $\alpha \to 0$ at infinity so that *both* the functions ϕ_1 and ϕ_2 tend to a constant value at infinity. Therefore neither of the profiles ϵ_+ and ϵ_- reflect waves at grazing incidence.

With these conditions, an entire family of these profiles can be generated. Two such examples are given in figures 4 and 5. To generate these HBS supporting profiles, we can choose any odd function $\alpha(x)$, with a value and derivative that goes to zero at $|x| = L/2$. The permittivity profiles derived from equation (9) then give us designs for dielectric materials that do not reflect TE waves at grazing incidence. Interestingly, with $\alpha(x)$ being an odd function, the permittivity profiles necessarily have regions where $\epsilon(x) < \epsilon_b$. This is immediately evident from our definition of the permittivity profiles in equation (9). After increasing in magnitude away from $x = -L/2$, $\alpha(x)$ must return to zero at $x = +L/2$. Therefore at some point the function $\alpha(x)$ must turn around, having finite value but zero gradient. At this point $\epsilon(x) - \epsilon_b = -\alpha^2 < 0$. In such regions the grazing wavevector in the direction of propagation, k_x becomes complex. In e.g. the WKB method, at the turning point where $\epsilon = \epsilon_b$, the wave is matched to a combination of Airy functions. In the case of a single turning point this gives rise to complete reflection [38]. The profiles found here have several turning points and run counter to this intuition, allowing complete transmission, despite the regions of exponential decay. Nevertheless the intuition is not completely wrong. The larger the region where $\epsilon(x)$ dips below ϵ_b, the larger the reflection is *close* to grazing incidence, and the narrower the range of angles close to $|\sin(\theta)|$ where the reflection vanishes. This effect can be seen in figure 4, where the comparatively large region of $\epsilon(x) < \epsilon_b$, leads to a mirror-like behaviour above $\gamma \sim 0.8$, and then a only a narrow angular range of low reflectivity around grazing incidence. As we shall see, when such profiles are realised as a multilayer, such narrow regions of low reflectivity will only be evident when the

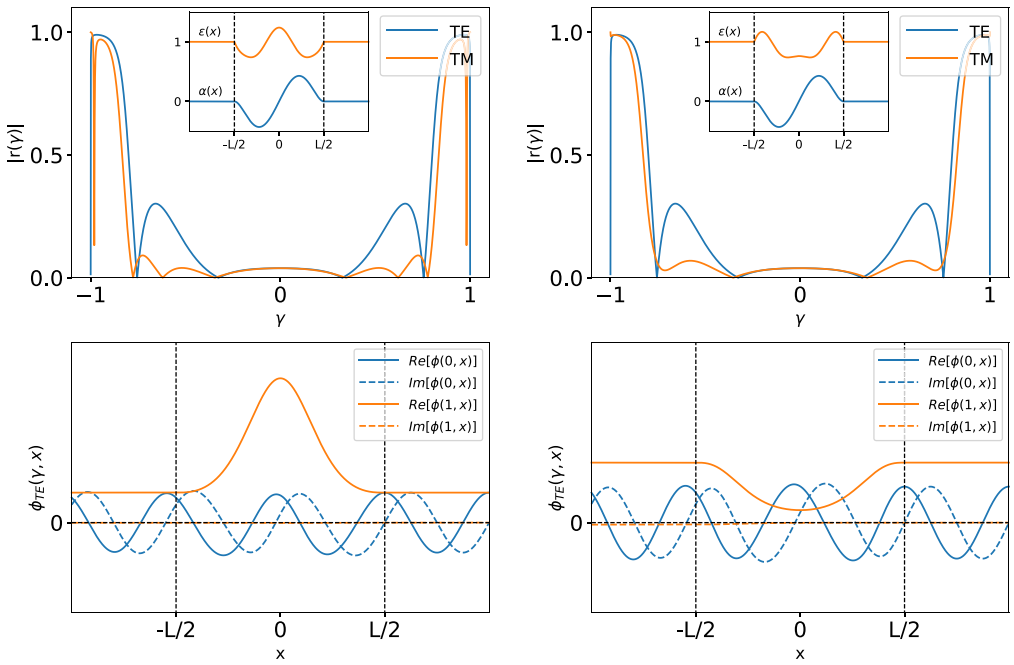

(a) The reflectivity (top) for a profile ϵ_+ generated from equation (9) (inset). The TE field (bottom) at both normal (blue) and grazing (orange) incidence.

(b) The reflectivity (top) for a profile ϵ_- generated from equation (9) (inset). The TE field (bottom) at both normal (blue) and grazing (orange) incidence.

Figure 4. The reflectivity profiles for the pair of permittivity profiles $\epsilon(x)$ found using equation (9) for $\alpha(x) = a_0(x/s)((x-L/2)/s)^2((x+L/2)/s)^2$a ($k_0 = 1, \lambda = 2\pi/k_0, a_0 = 1.5, s = \lambda, L = 2\lambda$). In both cases, there are large regions of $\epsilon(x) < 1$ which would be expected to cause extremely strong reflection as the angle of incidence increases. The onset of this strong reflection is evident beyond $\gamma \sim 0.8$ after which the reflectivity approaches unity. Rather surprisingly as the angle becomes close to grazing, this strong reflection rapidly decreases to zero. The TE fields shown in both cases again demonstrate that—in accordance with our design—at grazing incidence there is a mode that is constant outside the slab.

number of layers is large. Conversely in figure 5 the region where $\epsilon(x) < \epsilon_b$ is relatively small, resulting in a larger region of low reflectivity close to grazing incidence.

In practice such continuous permittivity profiles can be realised using a stack of N layers of fixed permittivity. Using the transfer matrix method [39] to compute the reflectivity, we now verify that for sufficiently large N the stack acts as predicted. Figure 6 shows that if the permittivity used in figure 5 is split into 25 fixed permittivity layers, the angle dependent reflectivity follows figure 5, dipping to the predicted low value as the wave approaches grazing incidence before then rising at extremely shallow angles of incidence. Devices with such low reflectivity close to grazing could have possible applications in the reduction of radar cross-sections, or removing glint from objects. In the case where the background permittivity is greater than 1 these profiles could be realised using a combination of low loss dielectrics (as in e.g. a rugate filter [40]), or at microwave frequencies using metamaterial building blocks [41, 42]. It is also worth noting that these profiles are not limited to EM materials, but could be realised with graded elastic media [43, 44].

3. Inversion of the Helmholtz equation

The factorization method is not the only way to find profiles that do not reflect grazing incidence waves. We now show that such designs can also be found via a direct inversion of the Helmholtz equation. This, for example allows us to have find complex permittivity profiles, and to modify the system's boundary conditions.

Take equation (3) with a background permittivity $\epsilon_b = 1$. Inverting the equation such that the permittivity is given as a function of the field, we obtain the simple equation

$$\epsilon(x) = 1 - \left(\frac{k_x}{k_0}\right)^2 - \frac{\phi''(x)}{k_0^2\phi(x)}, \tag{11}$$

where $\phi''(x)$ denotes the second derivative of the field w.r.t position. From our previous discussion we know that if, at grazing incidence the field is constant outside a profile which is symmetric in space, then the reflection vanishes. We note that while the solutions $\phi_{1,2}$ can be taken from our earlier equation (equation (10)) and inserted into the above equation (equation (11)) to yield $\epsilon_\pm$, in general the profiles derived from

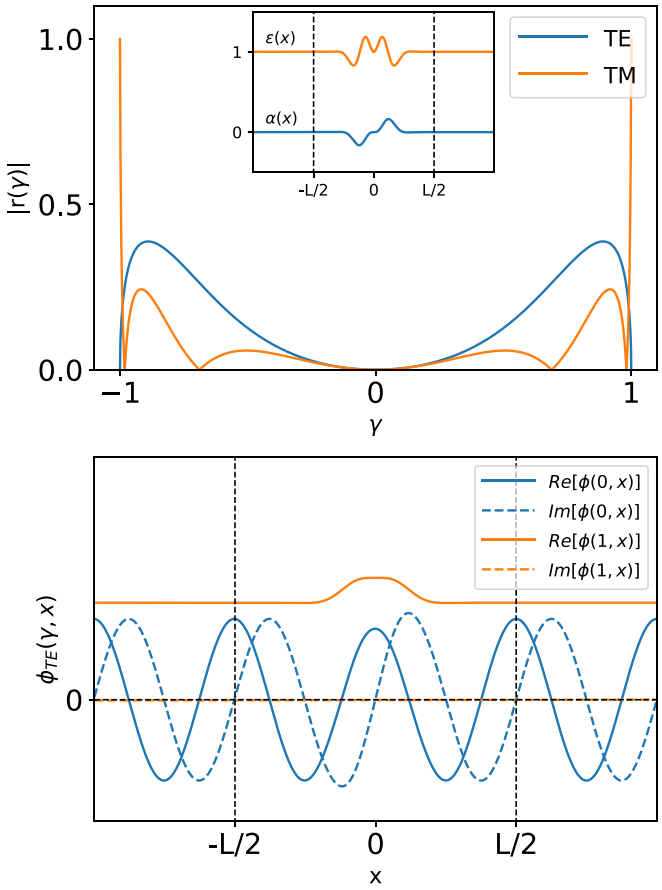

Figure 5. As in figure 4(a), for a different example $\alpha(x) = (x^2/a_0^4)\sin(x)\exp(-(1/a_0^2)x^2)$ profile (with the same k_0, λ, a_0 and L). In this case, $\alpha(x)$ is designed such that the region where $\epsilon_+(x) < 1$ is reduced. Accordingly the reflectivity reduces to zero over a greater angular range than in figure 4, as we approach grazing incidence.

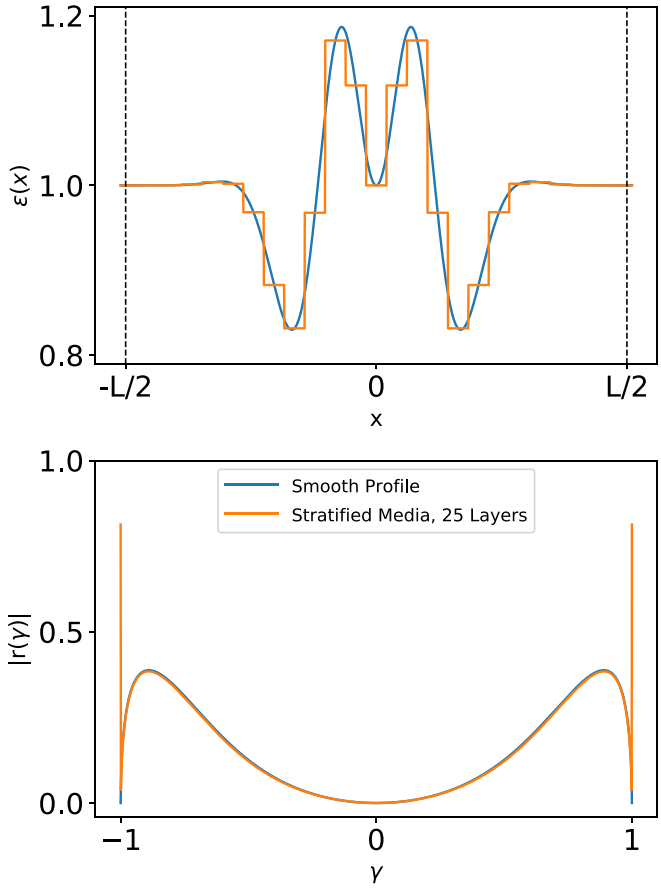

Figure 6. The permittivity profile plotted in figure 5 is split into a stack of 25 fixed index dielectrics (top). The reflectivity as a function of γ (bottom) is almost identical, with a region of low reflectivity close to grazing incidence. The effect of the discretization is to increase the reflectivity at extremely shallow angles of incidence.

the above equation will not obey equation (9), i.e. for the profiles equation (11) the Helmholtz equation will not necessarily be factorizable.

As a first example we assume the field profile is a Gaussian centred at $x = b$ with width a, plus a constant A

$$\psi(x) = A + \exp\left[-\left(\frac{x-b}{a}\right)^2\right]. \tag{12}$$

Provided $A \neq 0$, this function is a HBS. Inserting this into equation (11) with $k_x = 0$ we find the permittivity profile

$$\epsilon(x) = 1 - \left[\frac{4(x-b)^2 - 2a^2}{a^4 k_0^2 \left(A\exp\left[\left(\frac{x-b}{a}\right)^2\right] + 1\right)}\right]. \tag{13}$$

A numerical calculation of the reflectivity from this permittivity profile is given in figure 7. The TE reflectivity decays to zero at grazing incidence. There are again regions in the permittivity profile where $\epsilon(x) < 1$. These occur on the outer portions of the Gaussian where the second derivative ϕ'' is positive. Again we find profiles with regions where a wave at grazing incidence decays exponentially, but yet does not reflect. It is not however necessary for the permittivity to have such regions: it is possible to have $\phi''(x)/\phi(x) < 0$ everywhere, with zero gradient and non–zero value at $|x| = L/2$, as in the case of a homogeneous slab of constant permittivity where $\phi = \cos(k_0\sqrt{\epsilon - 1}x)$.

While it is interesting that there are a plethora of dielectric materials that do not reflect grazing incidence waves, in practice it would be useful to reduce grazing incidence reflection from an otherwise reflecting object. As an example, we consider applying the above theory to design an absorbing layer that when placed onto a mirror removes grazing incidence reflection at a fixed frequency $f = ck_0/2\pi$. We assume the following ansatz for the field

$$\phi(x) = \begin{cases} e^{ik_x x} & x < 0 \\ a(x-L) + b(x-L)^3 & 0 \leqslant x \leqslant L \\ 0 & x > L, \end{cases} \tag{14}$$

i.e. an incident wave at angle $k_x/k_0 = \cos(\theta)$ is completely absorbed in a layer of width L. The choice of the field inside the layer is a chosen such that the term $\phi''(x)/\phi(x)$ does not diverge at any x, and such that the field is zero on the mirror

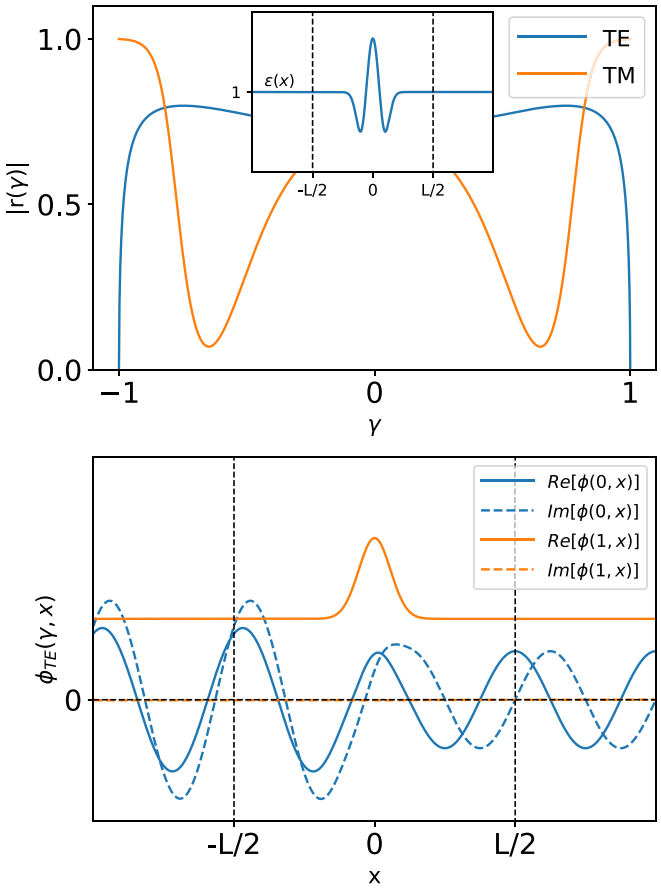

Figure 7. Reflectivity as a function of angle (top) for the permittivity profile equation (13) (inset) found through inversion of the Helmholtz equation at grazing incidence. The field (bottom) of the waves approaching at normal (blue) and grazing incidence (orange) show that as the angle approaches grazing incidence, the wave approaches the HBS equation (12).

at $x = L$. Continuity of the field and its first derivative at $x = 0$ gives the two constants a and b

$$a = \frac{-3 - \mathrm{i}k_x L}{2L}$$
$$b = \frac{1 + \mathrm{i}k_x L}{2L^3}. \tag{15}$$

Inserting equation (14) into equation (11) then yields, in the slab region

$$\epsilon(x) = 1 - \frac{6}{k_0^2} \frac{1}{(\frac{a}{b}) + (x - L)^2}$$
$$= 1 + \frac{3}{(k_0 L)^2} \frac{1}{\left(\frac{1 - \mathrm{i}k_x L}{1 + k_x^2 L^2}\right) + \frac{1}{2}\left[1 - \left(\frac{x}{L} - 1\right)^2\right]}, \tag{16}$$

with $\epsilon(x) = 1$ where $x < 0$. This complex profile removes reflection at a given angle θ, determined by $k_x/k_0 = \cos(\theta)$. The imaginary part of the profile represents the absorption required to eliminate the wave before it reaches the mirror, and is positive throughout the profile.

Figure 8 shows the reflectivity as a function of angle for the permittivity function equation (16) for the case of grazing

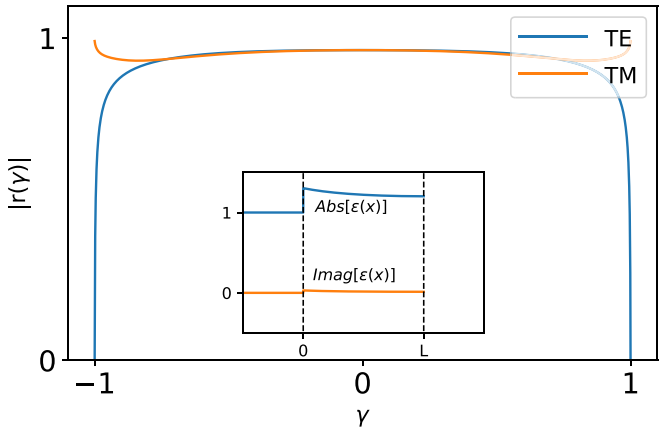

Figure 8. The geometry of the system is such that waves are incident from the left onto a dielectric material that is flanked by a perfect mirror. The reflectivity as a function of angle for the chosen permittivity function (equation (16)) is designed such that the reflection coefficient close to grazing incidence is zero.

incidence $k_x \approx 0$. Interestingly, in this limit the loss in the system becomes negligible and the profile tends to the limiting form $\epsilon(x) = 1 + 6(k_0 L)^{-2}[1 - (x/L - 1)^2]^{-1}$. This is paradoxical, as—due to energy conservation—away from grazing incidence the addition of a lossless layer to a mirror cannot give anything other than a phase shift to the reflected wave. The resolution to this paradox is that at grazing incidence the component of the Poynting vector normal to the mirror is zero, so we are not violating energy conservation. As the angle of zero reflection is brought towards grazing incidence, the loss in the profile diminishes. When the profile is to be reflectionless at exactly grazing incidence, we have a profile that has a reflectivity of unity except at exactly $k_x = 0$ where the dielectric acts as a waveguide with a confined mode that has an infinite decay constant in the region of free space outside. When k_x is close to zero the profile has a small amount of loss, which serves to absorb the wave and eliminate reflection close to grazing incidence. This shows that only a small amount of loss is required to eliminate the reflection of a wave where $k_x \sim 0$.

4. Conclusions

By factorizing the Helmholtz equation into a product of operators (as is done in supersymmetric quantum mechanics) we were able to design graded dielectric profiles that do not reflect TE polarized EM waves at grazing incidence. The physics behind this absence of reflection is analogous to the 'threshold' anomalies previously identified in one-dimensional quantum scattering, and occurs due to the presence of a zero 'energy' bound state within the profile. In electromagnetism we can understand these as waveguide modes that have an infinite decay constant, and our design procedure produces graded index waveguides with one mode that is on the boundary of being confined or radiative. This illustrates a new application of the formalism of supersymmetric quantum mechanics to the design of EM materials. The same approach could equally be applied to the TM polarization, if $\mu(x)$ was graded instead of

the permittivity $\epsilon(x)$. We found that the graded profiles derived in this way require regions where the permittivity is less than the background level ϵ_b. This is counter–intuitive, as such values usually imply strong reflection, leading to total internal reflection in the limit of an infinitely thick homogeneous slab.

In addition we also inverted the Helmholtz equation to obtain the permittivity in terms of the form of the wave at grazing incidence. From this we were again able to find similar profiles exhibiting a HBS as the incident wave approaches grazing. The inversion of the Helmholtz equation has the advantage that boundary conditions can be imposed on the wave. Imposing the vanishing of the wave amplitude at a single point, we found an absorbing graded index profile that can be added to the surface of a mirror to remove reflection at a particular angle. As the zero-reflection angle approaches grazing incidence the dissipation in the absorbing layer tends to zero, and there is an interesting regime where the reflection close to grazing is very small as is the dissipation in the layer.

Data availability statement

The data that support the findings of this study are available upon reasonable request from the authors.

Acknowledgments

The authors would like to acknowledge the Exeter Metamaterials CDT and the EPSRC (EP/L015331/1) for funding and supporting this research. SARH acknowledges financial support from a Royal Society TATA University Research Fellowship (RPG-2016-186).

ORCID iD

D A Patient https://orcid.org/0000-0001-9161-2114

References

[1] Oberst H, Kouznetsov D, Shimizu K, Fujita J-I and Shimizu F 2005 *Phys. Rev. Lett.* **94** 013203
[2] Compton A H 1923 *London, Edinburgh Dublin Phil. Mag. J. Sci.* **45** 1121
[3] DeWitt B T and Burnside W D 1988 *IEEE Trans. Ant. Prop.* **36** 971
[4] Collino F and Monk P B 1998 *Comput. Methods Appl. Mech. Eng.* **164** 157
[5] Landau L D and Lifshitz E M 1960 *Electrodynamics of Continuous Media* 1st edn (Oxford: Pergamon)
[6] Pöschl G and Teller E 1933 *Zeitschrift für Phys.* **83** 143
[7] Thekkekara L V, Achanta V G and Gupta S D 2014 *Opt. Exp.* **22** 17382
[8] Gardner C S, Greene J M, Kruskal M D and Miura R M 1967 *Phys. Rev. Lett.* **19** 1095
[9] Drazin P G and Johnson R S 1989 *Solitons: An Introduction* (Cambridge: Cambridge University Press)
[10] Horsley S A R 2016a *J. Opt.* **18** 085104
[11] Pendry J B 2000 *Phys. Rev. Lett.* **85** 3966
[12] Leonhardt U and Philbin T G 2006 *New J. Phys.* **8** 247
[13] Horsley S A R, Artoni M and La Rocca G C 2015 *Nat. Phot.* **9** 436
[14] Horsley S A R 2016b *Phys. Rev.* A **94** 063810
[15] Senn P 1988 *Am. J. Phys.* **56** 916
[16] Wigner E P 1948 *Phys. Rev.* **73** 1002
[17] Levinson N 1949 *Kgl. Danske Videnskab. Selskab Mat.-fys. Medd.* **25** 9
[18] Zhong-Qi M 2006 *J. Phys. A: Math. Gen.* **39** R625
[19] Wellner M 1964 *Am. J. Phys.* **32** 787
[20] Cooper F, Khare A and Sukhatme U P 1995 *Phys. Rep.* **251** 267
[21] Borghi R 2017 *Eur. J. Phys.* **38** 025404
[22] Chumakov S M and Wolf K B 1994 *Phys. Lett.* A **193** 51
[23] Miri M-A, Heinrich M, El-Ganainy R and Christodoulides D N 2013 *Phys. Rev. Lett.* **110** 233902
[24] Longhi S and Della Valle G 2013 *EPL* **102** 40008
[25] Yu S, Piao X, Hong J and Park N 2015 *Nat. Commun.* **6** 8269
[26] Miri M A, Heinrich M and Christodoulides D N 2014 *Optica* **1** 89
[27] García-Meca C, Ortiz A M and Sáez R L 2020 *Nat. Commun.* **11** 1
[28] Cortés L F O and García N F 2014 *J. Phys. Conf. Ser.* **512** 012027
[29] Demić A, Milanović V and Radovanović J 2015 *Phys. Lett. A* **379** 2707
[30] Macho A, Llorente R and García-Meca C 2018 *Phys. Rev. Appl.* **9** 014024
[31] Nogami Y and Ross C K 1996 *Am. J. Phys.* **64** 923
[32] Newton R G 2002 *Scattering Theory of Waves and Particles* (New York: Dover)
[33] Virtanen P *et al* 2020 *Nat. Methods* **17** 261
[34] Ahmed Z *et al* 2017 *Eur. J. Phys.* **38** 025401
[35] van Dijk W and Nogami Y 2017 *Eur. J. Phys.* **38** 038002
[36] Ahmed Z, Kumar S and Sharma D 2020 (arXiv:2005.03721)
[37] Ahmed Z, Sharma D, Kaiwart R and Irfan M 2017 (arXiv:1612.07081v2)
[38] Heading J 2013 *An Introduction to Phase-Integral Methods* (New York: Dover)
[39] Born M and Wolf E 2013 *Principles of Optics* (Amsterdam: Elsevier)
[40] Gunning W J, Hall R L, Woodberry F J, Southwell W H and Gluck N S 1989 *Appl. Opt.* **28** 2945
[41] Smith D R, Mock J J, Starr A F and Schurig D 2005 *Phys. Rev.* E **71** 036609
[42] Della Giovampaola C and Engheta N 2014 *Nat. Mat.* **13** 1115
[43] Sepehri S, Jafari H, Mashhadi M M, Yazdi M R H and Fakhrabadi M M S 2020 *Acta Mech.* **231** 3363
[44] Carcione J M and Cavallini F 1995 *Wave Motion* **21** 149